

Influence of Molecular Design on Radical Spin Multiplicity: Characterisation of BODIPY Dyad and Triad Radical Anions.

Barry Mangham, Magnus W. D. Hanson-Heine, E. Stephen Davies, Alisdair Wriglesworth, Michael W. George, William Lewis, Deborah L. Kays, Nicholas A. Besley, and Neil R. Champness*

Supporting Information Table of Contents

Experimental Details	Page 1-4
Electrochemical and Spectroelectrochemical Measurements	Page 4-5
Single Crystal X-Ray Diffraction Studies	Page 5
DFT Calculations	Page 6
Supplementary Figures for Cyclic Voltammetry	Page 7-9
Supplementary Figures for EPR spectroscopy	Page 9
Supplementary Figures for UV/vis Spectroelectrochemistry	Page 10-13
Supplementary Figures for Fluorescence Spectroscopy	Page 13
DFT Geometry Optimized Structures and MO diagrams	Page 14-18
Representation of quinoidal structures of radical anions	Page 18
References for Supporting Information	Page 19

Further Experimental Details

4-(4,4,5,5-tetramethyl-1,3,2-dioxaborolan-2-yl)benzaldehyde was prepared from 4-boronic acid benzaldehyde following literature procedures.^{S1} 1,3,5-tris(formyl)benzene was prepared following literature procedures from 1,3,5-tris(carboxy)benzene via esterification with MeOH in the presence of sulphuric acid to give 1,3,5-tris(methoxycarbonyl)benzene, 96 % yield,^{S2} followed by reduction with LiAlH₄ to give the corresponding 1,3,5-tris(hydroxy)benzene in 99 % yield^{S3} and then selective oxidation with pyridinium chlorochromate to afford 1,3,5-tris(formyl)benzene in 45 % yield.^{S4} 4,4'-bis(dicarbaldehyde)biphenyl was prepared according to literature procedures.^{S5} 1,4-bis(bromomethyl)durene was prepared by bromomethylation of durene^{S6} followed by treatment with potassium hydroxide and 2-nitropropane give the product in 73 % yield.^{S7}

Synthesis of terphenyl-4,4'-dicarbaldehyde; A mixture of 4-(4,4,5,5-tetramethyl-1,3,2-dioxaborolan-2-yl)benzaldehyde (2.50 g, 10.8 mmol) and 1,4-dibromobenzene (1.27 g, 5.4 mmol) in sodium carbonate solution (2M, 17 ml) and 1,4-dioxane (170 ml) was degassed under dinitrogen. After 2 hours tetrakis(triphenylphosphine)palladium (0.30 g, 0.26 mmol) was added and the reaction mixture was heated to reflux. After 24 hours the reaction mixture was cooled to room temperature and solvent removed under reduced pressure. Dichloromethane (150 ml) was added to the resulting brown solid and organics were washed with water (3 x 100 ml), dried over sodium sulfate and solvent removed under reduced pressure. The resulting brown solid was purified by column chromatography [silica, dichloromethane] to give a white solid in 49 % yield (0.76 g, 2.65 mmol). ¹H NMR (CDCl₃, 400 MHz) δ = 10.09 (s, 2H), 8.00 (d, *J*=8.2 Hz, 4H), 7.83 (d, *J*=8.2 Hz, 4H), 7.78 (s, 4H). ¹³C NMR (CDCl₃, 100 MHz) δ = 191.83, 146.24, 139.75, 135.44, 130.36, 127.97, 127.61. Elemental analysis calculated for C₂₀H₁₄O₂: C, 83.90; H, 4.93 found: C, 83.83; H, 4.98.

General experimental procedure for bis-substituted dipyrromethanes

Aldehyde (15.0 mmol) was stirred in pyrrole (150 ml, 2.16 mol) with degassing under dinitrogen at room temperature. After 20 minutes trifluoroacetic acid (0.8 ml, 10.4 mmol) was added. After 5 minutes sodium hydroxide (0.82 g, 20.5 mmol) was added. After 10 minutes the reaction mixture was filtered and solvent removed under reduced pressure. The resulting solid was purified by column chromatography [silica, dichloromethane], unless otherwise stated.

Synthesis of 1,4-bis(dipyrromethane-5-yl)benzene; obtained as an off white solid in 77 % yield (4.20 g, 11.5 mmol). ¹H NMR (CDCl₃, 400 MHz) δ = 7.95 (br. s, 4H), 7.18 (s, 4H), 6.71 (m, 4H), 6.16 (m, 4H), 5.93 (m, 4H), 5.47 (s, 2H). ¹³C NMR (CDCl₃, 100 MHz) δ = 140.80, 132.37, 128.60, 117.24, 108.43, 107.19, 43.64. MS: (+ve ESI) m/z calculated for C₂₄H₂₂N₄Na [M + Na]⁺: 389.1742, found: 389.1746.

Synthesis of 1,3-bis(dipyrromethane-5-yl)benzene; obtained as a light brown solid in 80 % yield (4.41 g, 12.1 mmol). ¹H NMR (CDCl₃, 400 MHz) δ = 7.89 (br. s, 4H), 7.28 (m, 1H), 7.12 (m, 3H), 6.68 (s, 4H), 6.15 (s, 4H), 5.89 (s, 4H), 5.40 (s, 2H). ¹³C NMR (CDCl₃, 100 MHz) δ = 142.42, 132.42, 128.86, 128.52, 126.86, 117.64, 117.31, 108.29, 108.10, 107.68, 107.19, 103.67, 43.78. MS: (+ve ESI) m/z calculated for C₂₄H₂₂N₄Na [M + Na]⁺: 389.1742, found: 389.1733.

Synthesis of 1,4-bis(dipyrromethane-5-yl)durene; obtained as a pale yellow solid in 20 % yield (1.28 g, 3.02 mmol). ¹H NMR (CDCl₃, 400 MHz) δ = 8.00 (br. s, 4H), 6.71 (s, 4H), 6.21 (q, J=2.8x(3) Hz, 4H), 6.09 (s, 2H), 6.03 (s, 4H), 2.07 (s, 12H). ¹³C NMR (CDCl₃, 100 MHz) δ = 137.04, 131.82, 116.19, 108.64, 106.26, 39.55, 17.53. MS: (+ve ESI) m/z calculated for C₂₈H₃₁N₄ [M + H]⁺: 423.2549, found: 423.2544. Elemental analysis calculated for C₂₄H₂₄O₆: C, 79.59; H, 7.16; N, 13.26, found: C, 79.47; H, 7.18; N, 13.10.

Synthesis of 4,4'-bis(dipyrromethane-5-yl)biphenyl; recrystallised from dichloromethane/hexane to give an off-white solid in 75 % yield (4.97 g, 11.2 mmol). ¹H NMR (DMSO-d₆, 400 MHz) δ = 10.58 (s, 4H), 7.53 (d, J=8.3 Hz, 4H), 7.21 (d, J=8.3 Hz, 4H), 6.61 (m, 4H), 5.90 (m, 4H), 5.70 (m, 4H), 5.37 (s, 2H). ¹³C NMR (DMSO-d₆, 100 MHz) δ = 142.93, 137.91, 132.94, 128.56, 126.23, 116.84, 106.85, 106.05, 43.09. MS: (+ve ESI) m/z [M+Na⁺] calcd C₃₀H₂₆N₄Na: 465.2055, found: 465.2063.

Synthesis of 4,4'-bis(di(1H-pyrrol-2-yl)methyl)terphenyl; This compound was prepared on a smaller scale as follows. A solution of terphenyl-4,4'-dicarbaldehyde (0.50 g, 1.75 mmol) in pyrrole (40 ml, 0.58 mol) was degassed under dinitrogen with shielding from light. After 20 minutes indium trichloride (0.10 g, 0.45 mmol) was added. After 1.5 hours sodium hydroxide (35 mg, 0.90 mmol) was added. After a further 1.5 hours the reaction mixture was filtered and solvent removed under reduced pressure. The resulting off-white solid was recrystallised from ethyl acetate/hexane to give a white solid in 71 % yield (0.64 g, 1.24 mmol). ¹H NMR (CDCl₃, 400 MHz) δ = 10.70 (s, 4H), 7.71 (s, 4H), 7.62 (d, J=8.3 Hz, 4H), 7.27 (d, J=8.3 Hz, 4H), 6.63 (m, 4H), 5.93 (m, 4H), 5.74 (s, 4H), 5.42 (s, 2H). ¹³C NMR (CDCl₃, 100 MHz) δ = 143.28, 138.83, 137.43, 132.94, 128.66, 126.98, 126.22, 116.88, 106.85, 106.05, 43.12. MS: (+ve ESI) m/z [M + Na⁺] calcd C₃₆H₃₀N₄Na: 541.2368, found: 541.2344.

Synthesis of 1,3,5-tris(dipyrromethane-5-yl)benzene: 1,3,5-triformylbenzene (0.54 g, 3.33 mmol) was stirred in pyrrole (50 ml, 0.72 mol) under nitrogen. After 10 minutes trifluoroacetic acid (0.32 ml, 4.18 mmol) was added. After 5 minutes sodium hydroxide (0.32 g, 8.00 mmol) was added. After a further 5 minutes the reaction mixture was filtered and solvent was removed under reduced pressure. The

resulting dark blue solid was purified by column chromatography [silica, dichloromethane/ethyl acetate (4:1)] to give a pale yellow solid in 87 % yield (1.49 g, 2.92 mmol). ^1H NMR (CDCl_3 , 400 MHz) δ = 7.72 (br. s, 3H), 6.95 (s, 6H), 6.59 (s, 6H), 6.10 (d, $J=2.6$ Hz, 6H), 5.78 (s, 6H), 5.11 (br. s, 3H). ^{13}C NMR (CDCl_3 , 100 MHz) δ = 142.78, 133.33, 126.25, 116.53, 106.82, 105.98, 43.75. MS: (ESI) m/z calculated for $\text{C}_{33}\text{H}_{30}\text{N}_6\text{Na}$ [$\text{M} + \text{Na}$] $^+$: 533.2430, found: 533.2423. Elemental analysis for $\text{C}_{33}\text{H}_{30}\text{N}_6$: C, 77.62; H, 5.92; N, 16.46. Found: C, 77.48; H, 5.90; N, 16.28.

General experimental procedure for BODIPY dyads and triad

2,3-Dichloro-5,6-dicyano-1,4-benzoquinone (0.25 g, 1.10 mmol) in anhydrous toluene (10 ml) was added to a stirred solution of selected dipyrromethane (0.55 mmol) in anhydrous toluene (20 ml) under dinitrogen. After 5 minutes *N,N*-diisopropylethylamine (1.5 ml, 6.31 mmol) and boron trifluoride diethyl etherate (1.0 ml, 8.10 mmol) were added. After 1 hour the solvent was removed under reduced pressure.

Synthesis of 1: purified by column chromatography [silica, dichloromethane/hexane (1:1)] to give a red solid in 8 % yield (20 mg, 0.04 mmol). ^1H NMR (CDCl_3 , 400 MHz) δ = 8.02 (s, 4H), 7.77 (s, 4H), 7.01 (d, $J=4.2$ Hz, 4H), 6.62 (d, $J=3.2$ Hz, 4H). ^{13}C NMR (CDCl_3 , 100 MHz) δ = 145.40, 144.94, 136.12, 134.74, 131.44, 130.48, 119.02. ^{11}B NMR (CDCl_3 , 128 MHz) δ = 0.28 (t, $J=28.2 \times (2)$ Hz). ^{19}F NMR (CDCl_3 , 377 MHz) δ = -144.97 (q, $J=30.2 \times (3)$ Hz). MS: (MALDI-TOF, DCTB/MeCN) m/z calculated for $\text{C}_{24}\text{H}_{16}\text{B}_2\text{F}_4\text{N}_4$ [M] $^+$: 458.0, found: 457.9.

Synthesis of 2: purified by column chromatography [silica, dichloromethane/hexane (4:1)] to give a red solid in 6 % yield (14 mg, 0.03 mmol). ^1H NMR (CDCl_3 , 400 MHz) δ = 7.99 (s, 4H), 7.77 (m, 4H), 6.95 (d, $J=4.3$ Hz, 4H), 6.60 (d, $J=4.1$ Hz, 4H). ^{13}C NMR (CDCl_3 , 100 MHz) δ = 145.22, 144.96, 134.77, 134.20, 132.40, 131.83, 131.30, 128.75, 119.09. ^{11}B NMR (CDCl_3 , 128 MHz) δ = 0.25 (t, $J=29.4 \times (2)$ Hz). ^{19}F NMR (CDCl_3 , 377 MHz) δ = -144.93 (q, $J=30.2 \times (3)$ Hz). MS: (MALDI-TOF, DCTB/MeCN) m/z calculated for $\text{C}_{24}\text{H}_{16}\text{B}_2\text{F}_4\text{N}_4$ [M] $^+$: 458.0, found: 457.9.

Synthesis of 4: purified by column chromatography [silica, dichloromethane/hexane (1:1)] to give a red solid in 11 % yield (30 mg, 0.06 mmol). ^1H NMR (CDCl_3 , 400 MHz) δ = 7.98 (s, 4H), 6.71 (d, $J=4.0$ Hz, 4H), 6.54 (d, $J=3.1$ Hz, 4H), 2.10 (s, 12H). ^{11}B NMR (CDCl_3 , 128 MHz) δ = 0.35 (t, $J=28.2 \times (2)$ Hz). ^{19}F NMR (CDCl_3 , 377 MHz) δ = -145.62 (q, $J=28.7 \times (3)$ Hz). MS: (MALDI-TOF, DCTB/MeCN) m/z calculated for $\text{C}_{28}\text{H}_{24}\text{B}_2\text{F}_4\text{N}_4$ [M] $^+$: 514.2, found: 514.3.

Synthesis of 5: purified by column chromatography [silica, dichloromethane] to give an orange solid in 7 % yield (20 mg, 0.04 mmol). ^1H NMR (CDCl_3 , 400 MHz) δ = 7.99 (s, 4H), 7.85 (d, $J=8.0$ Hz, 4H), 7.74 (d, $J=8.2$ Hz, 4H), 7.03 (d, $J=3.6$ Hz, 4H), 6.60 (d, $J=2.6$ Hz, 4H). ^{13}C NMR (CDCl_3 , 100 MHz) δ = 146.61, 144.32, 142.25, 134.87, 133.62, 131.47, 131.31, 127.22, 118.67. ^{11}B NMR (CDCl_3 , 128 MHz) δ = 0.29 (t, $J=28.2 \times (2)$ Hz). ^{19}F NMR (CDCl_3 , 377 MHz) δ = -144.93 (q, $J=28.7 \times (3)$ Hz). MS: (MALDI-TOF, DCTB/MeCN) m/z calculated for $\text{C}_{30}\text{H}_{20}\text{B}_2\text{F}_4\text{N}_4$ [M] $^+$: 534.2, found: 534.3.

Synthesis of 6: purified by column chromatography [silica, dichloromethane] followed by PTLC [silica, dichloromethane/hexane (3:2)] to give an orange solid in 7 % yield (22 mg, 0.04 mmol). ^1H NMR (CDCl_3 , 400 MHz) δ = 7.99 (br. s, 4H), 7.85 (m, 8H), 7.72 (d, $J=8.3$ Hz, 4H), 7.05 (d, $J=4.1$ Hz, 4H), 6.60 (d, $J=3.0$ Hz, 4H). ^{13}C NMR (CDCl_3 , 100 MHz) δ = 146.93, 144.15, 142.93, 139.53, 134.87, 133.05, 131.49, 131.25,

127.83, 127.02, 118.60. ^{11}B NMR (CDCl_3 , 128 MHz) $\delta = 0.33$ (t, $J=28.2 \times (2)$ Hz). ^{19}F NMR (CDCl_3 , 377 MHz) $\delta = -145.0$ (q, $J=28.7 \times (3)$ Hz). MS: (MALDI-TOF, DCTB/MeCN) m/z calculated for $\text{C}_{36}\text{H}_{24}\text{B}_2\text{F}_4\text{N}_4$ $[\text{M}]^+$: 610.2, found: 610.3.

Synthesis of 3: 2,3-Dichloro-5,6-dicyano-1,4-benzoquinone (0.35 g, 1.54 mmol) in anhydrous toluene (20 ml) was added to a stirred solution of 1,3,5-tris(dipyrrromethan-5-yl)benzene (0.50 g, 0.98 mmol) in anhydrous toluene (50 ml) at room temperature. After 5 minutes *N,N*-diisopropylethylamine (6.0 ml, 34.4 mmol) and boron trifluoride diethyl etherate (6.0 ml, 48.6 mmol) were added. After 1 hour water (100 ml) was added, organics were separated, dried over magnesium sulphate and solvent removed under reduced pressure. The resulting brown solid was purified by column chromatography [silica, dichloromethane] to give a red solid in 3 % yield (17 mg, 0.03 mmol). ^1H NMR (CDCl_3 , 400 MHz) $\delta = 8.04$ (br. s, 6H), 8.03 (s, 3H), 6.96 (d, $J=4.1$ Hz, 6H), 6.64 (d, $J=3.3$ Hz, 6H). ^{13}C NMR (CDCl_3 , 100 MHz) $\delta = 145.75$, 143.29, 134.78, 134.61, 133.53, 131.03, 119.62. ^{11}B NMR (CDCl_3 , 128 MHz) $\delta = 0.23$ (t, $J=28.2 \times (2)$ Hz). ^{19}F NMR (CDCl_3 , 377 MHz) $\delta = -144.98$ (q, $J=30.2 \times (3)$ Hz). MS: (MALDI-TOF, DCTB/MeCN) m/z calculated for $\text{C}_{33}\text{H}_{20}\text{B}_3\text{F}_6\text{N}_6$ $[\text{M} - \text{H}]^-$: 647.2, found: 647.4.

Electrochemical and Spectroelectrochemical Measurements

UV/visible absorption spectra were recorded on a Perkin-Elmer Lambda 25 spectrometer.

Cyclic voltammetric studies were carried out using either an Autolab PGSTAT20 or an Autolab PGSTAT302N potentiostat. Standard cyclic voltammetry was carried out under an atmosphere of argon using a three-electrode arrangement in a single compartment cell. A glassy carbon working electrode, a Pt wire secondary electrode and a saturated calomel reference electrode, chemically isolated from the test solution via a bridge tube containing electrolyte solution and fitted with a porous vycor frit, were used in the cell. The solutions were 10^{-3} M in test compound and 0.4 M in $[\text{Bu}_4][\text{BF}_4]$ as supporting electrolyte. Redox potentials are quoted versus the ferrocenium–ferrocene couple used as an internal reference. Compensation for internal resistance was not applied.

Bulk electrolysis experiments, at a controlled potential, were carried out using a two-compartment cell. The Pt/Rh gauze basket working electrode was separated from the wound Pt/Rh gauze secondary electrode by a glass frit. A saturated calomel reference electrode was bridged to the test solution through a vycor frit orientated at the centre of the working electrode. The working electrode compartment was fitted with a magnetic stirrer bar and the test solution was stirred rapidly during electrolysis. The solutions used were 0.4 M in $[\text{Bu}_4][\text{BF}_4]$ as supporting electrolyte and 10^{-3} M in test compound and were prepared using Schlenk line techniques. Electrolysed solutions were transferred to quartz tubes, via teflon cannula, for analysis by EPR spectroscopy. EPR spectra were recorded on a Bruker EMX spectrometer fitted with an X-band microwave bridge as fluid solutions (at room temperature) and as frozen glasses (at 77 K) using a microwave power of ca. 20 mW. Spectra were simulated using WINEPR SimFonia (Shareware version 1.25, Brüker Analytische Messtechnik GmbH).

The UV/vis spectroelectrochemical experiments were carried out with an optically transparent electrochemical (OTE) cell (modified quartz cuvette, optical pathlength: 0.5 mm). A three-electrode configuration, consisting a Pt/Rh gauze working electrode, a Pt wire secondary electrode (in a fritted PTFE sleeve) and a saturated calomel electrode, chemically isolated from the test solution via a bridge

tube containing electrolyte solution and terminated in a porous frit, was used in the cell. The potential at the working electrode was controlled by a Sycopel Scientific Ltd DD10M potentiostat. The UV/vis spectra were recorded on a Perkin Elmer Lambda 16 spectrophotometer. The cavity was purged with dinitrogen and temperature control at the sample was achieved by flowing cooled dinitrogen across the surface of the cell.

Single Crystal X-Ray Diffraction Studies

Single-crystal X-ray diffraction experiments were performed on either a Bruker AXS SMART APEX CCD area detector diffractometer (**2**) equipped with an Oxford Cryosystems open flow cryostat operating at 90 K using graphite-monochromated Mo K α radiation ($\lambda = 0.71073 \text{ \AA}$), a Rigaku Saturn 724+ CCD area detector on a Crystal Logic 4-circle kappa goniometer, mounted on Beamline I19 at the UK (**1,3**). Using Olex2,⁵⁸ the structure was solved with the ShelXT⁵⁹ structure solution program using Intrinsic Phasing and refined with the ShelXL⁵¹⁰ refinement package using Least Squares minimisation. For specific details of modelling of disorder see cifs for each structure.

Crystal data for 1: C₂₄H₁₆B₂F₄N₄. Monoclinic, space group *P*2₁/*c* (No. 14), *a* = 6.0437(4), *b* = 11.6835(7), *c* = 14.5203(10) Å, *V* = 1019.03(12) Å³, *T* = 100(2) K, *Z* = 2, *D*_{calc} = 1.493 g cm⁻³, μ = 0.115 mm⁻¹, *F*(000) = 468.0. Final *R*₁ (*wR*₂) = 0.033 (0.089) with GOF = 1.073.

Crystal data for 2: C₂₄H₁₆B₂F₄N₄. Monoclinic, space group *C*₂/*c* (No. 15), *a* = 19.818(14), *b* = 10.284(5), *c* = 12.947(6) Å, *V* = 2005(2) Å³, *T* = 90 K, *Z* = 4, *D*_{calc} = 1.517 g cm⁻³, μ = 0.116 mm⁻¹, *F*(000) = 936.0. Final *R*₁ (*wR*₂) = 0.054 (0.137) with GOF = 1.147.

Crystal data for 3: C₃₃H₂₁B₃F₆N₆·0.5(CH₂Cl₂) Monoclinic, space group *P*2₁/*c* (No. 14), *a* = 20.50(2), *b* = 20.40(2), *c* = 8.110(8) Å, β = 95.68°, *V* = 3375(6) Å³, *T* = 120 K, *Z* = 4, *D*_{calc} = 1.359 g cm⁻³, μ = 0.141 mm⁻¹, *F*(000) = 1404. Final *R*₁ (*wR*₂) = 0.133 (0.373) with GOF = 1.304.

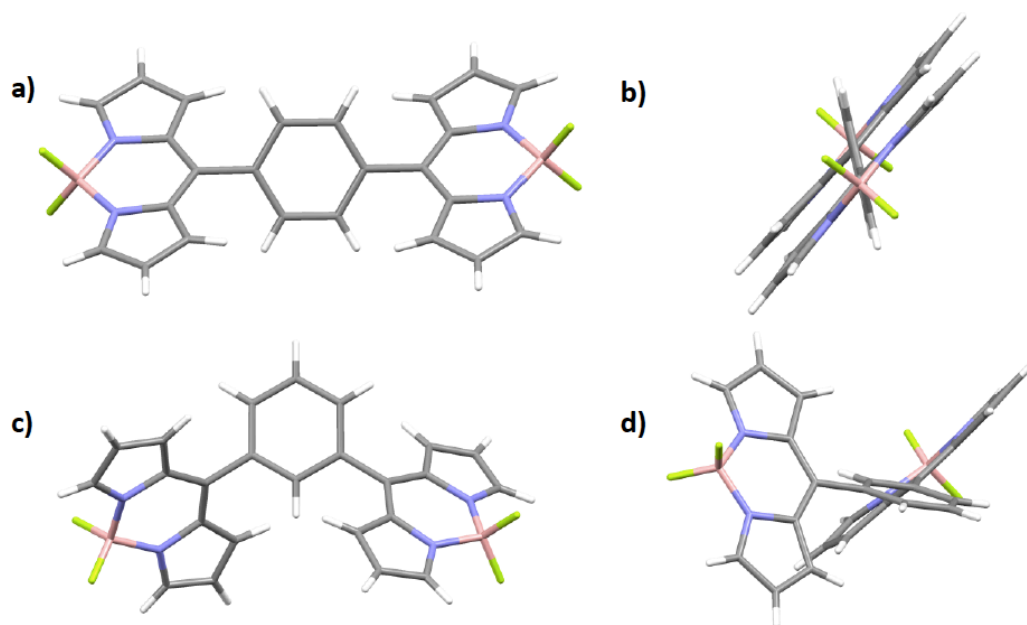


Figure S1. Views of the single crystal X-ray structures for **1** a) and b); **2** c) and d). Colour guide: boron (pink), fluorine (yellow), nitrogen (blue), carbon (grey), hydrogen (white).

DFT Calculations

The structure of the neutral and reduced forms of the molecules was optimized using Kohn-Sham density functional theory (DFT) with the ω B97M-V functional^{S11} and the 6-311G* basis set. For the di-reduced species the open-shell singlet state was studied by using the maximum overlap method^{S12} to maintain the correct orbital occupancies during the DFT calculation. Absorption spectra were calculated using time-dependent density functional theory (TDDFT) within the Tamm-Dancoff approximation^{S13} using the same functional and basis set. A Λ analysis^{S14} was performed to confirm that a hybrid functional is suitable to describe the electronic transitions. The calculations of the spectra used a polarized continuum solvent model^{S15} with a dielectric constant of 80.0. The computed spectra are represented by convoluting the calculated energies and oscillator strengths with Gaussian functions with a full-width at half maximum of 20 nm. To facilitate comparison with the experimental data, an energy shift has been applied to the computed spectra. The magnitude of this shift corresponds to the energy shift required to align the low energy band of the neutral compound with experiment. This shift is then applied to all subsequent spectra for the compound. All calculations were performed with the Q-Chem software package.^{S16} The energy of the open-shell singlet states cannot be determined reliably with Kohn-Sham DFT since this a single reference based method and the open-shell states have multi-determinant character. The energies of the di-reduced species were also computed using second-order multireference perturbation theory^{S17} with the MOLPRO software package.^{S18} These calculations used an active space which contained the BODIPY based π and π^* orbitals (HOMO-1, HOMO, LUMO and LUMO+1) and the 6-311G basis set.

Supplementary Figures for Cyclic Voltammetry and Spectroelectrochemistry

Table S1. Summary of square wave voltammetry data, absorption wavelengths (λ_{abs}) and extinction coefficients (ϵ) for both neutral and reduced, dianionic or trianionic, species for compounds **1-6**.^a

Compound	$E_{1/2}/V$ (ΔE)	$\lambda_{\text{abs}}/\text{nm}$ ($\epsilon \times 10^{-4}/\text{dm}^3 \text{ mol}^{-1} \text{ cm}^{-1}$)	
		Neutral Species	Radical anions [1] ²⁻ , [2] ²⁻ , [3] ³⁻ , [4] ²⁻ , [5] ²⁻ , [6] ²⁻
1	-1.03	278 (0.5), 363 (3.3), 507 (10.1)	274 (1.2), 417 (0.8), 554 (4.4), 665 (2.2)
2	-1.10 -1.22	232 (2.4), 272 (0.5), 347 (2.4), 503 (9.0),	294 (1.8), 338 (2.7), 475 (0.7), 506 (1.3), 539 (2.3)
3	-1.02 -1.14 -1.27	340 (3.3), 507 (10.5),	293 (2.2), 337 (3.2), 378 (2.2), 475 (0.7), 504 (1.4), 537 (2.6)
4	-1.22 -1.31	237 (6.5), 304 (0.9), 356 (1.4), 480 (5.4), 500 (11.7)	226 (2.9), 288 (2.4), 338 (2.1), 474 (0.3), 500 (1.1), 531 (1.8)
5	-1.17	250 (2.4), 389 (2.6), 504 (8.7)	268 (1.7), 304 (2.0), 340 (2.1), 412 (1.1), 504 (1.0), 537 (1.7), 686 (1.6)
6	-1.16	277 (2.9), 409 (3.1), 503 (10.7)	292 (3.0), 340 (2.6), 423 (2.0), 478 (0.7), 509 (1.5), 544 (2.3), 626 (0.7)

^a In CH_2Cl_2 containing [$n\text{Bu}_4\text{N}$][BF_4] (0.4 M); ^b at 243 K;

Table S2. Effect of scan rate on ΔE ($= E_p^a - E_p^c$), in mV, for the reduction of compounds **1**, **5** and **6** and corresponding values (in brackets) for the ferrocenium/ferrocene couple used as the internal standard

Scan rate / Vs ⁻¹	1	5	6
0.02	52 (68)	89 (71)	72 (73)
0.05	58 (69)	89 (73)	75 (73)
0.10	66 (72)	93 (77)	79 (76)
0.20	76 (74)	97 (79)	83 (78)
0.30	84 (76)	100 (83)	89 (82)

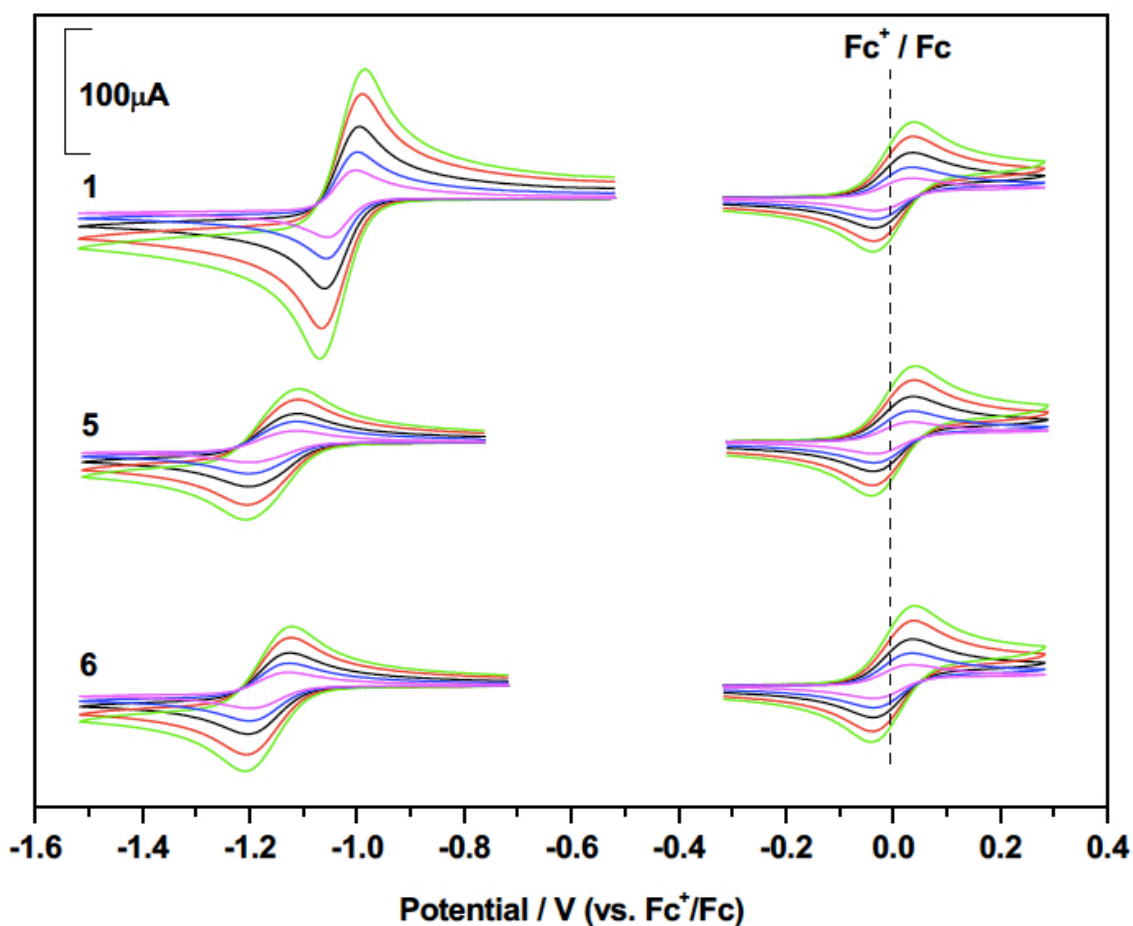


Figure S2. Effect of scan rate on the peak separations for **1**, **5**, **6** and ferrocene. Scan rates of 0.02, 0.05, 0.10, 0.20 and 0.30 Vs⁻¹ are shown in magenta, blue, black, red and green, respectively.

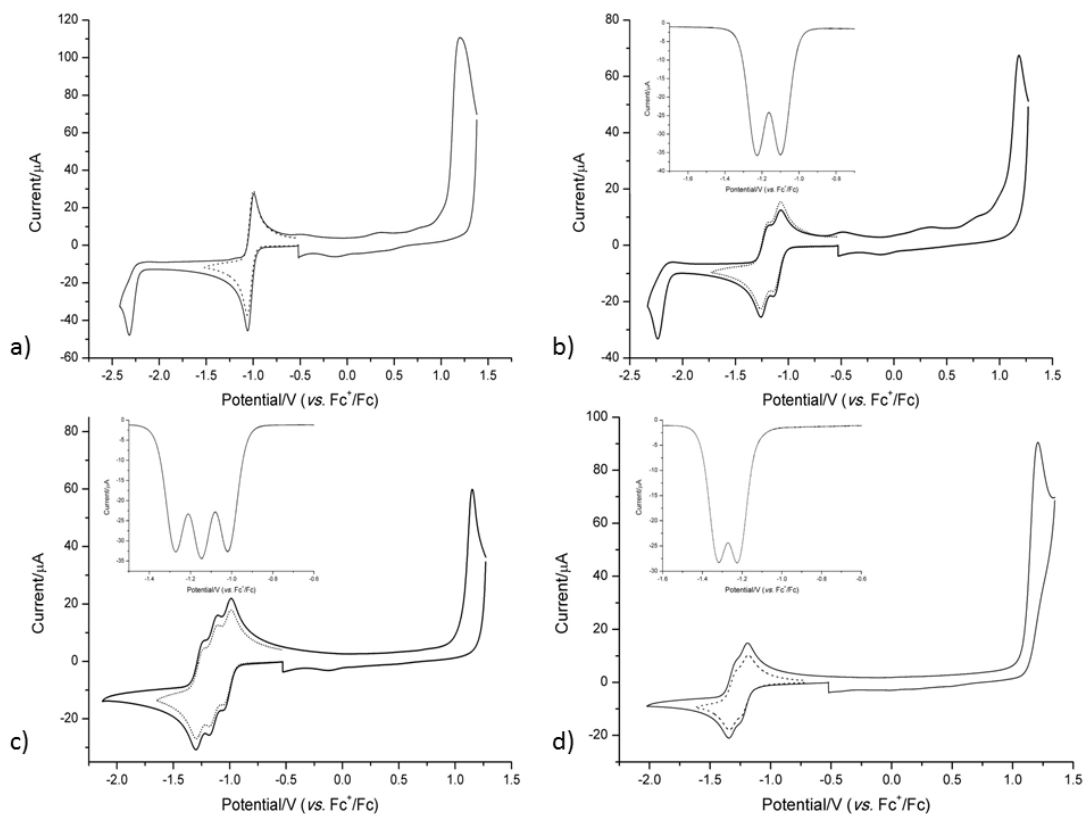


Figure S3. Cyclic voltammograms of a) **1**, b) **2**, c) **3** and d) **4** recorded at RT in CH_2Cl_2 with $[\text{nBu}_4\text{N}][\text{BF}_4]$ (0.4 M) as supporting electrolyte. Insets in b), c) and d): square wave voltammetry indicating multiple independent but overlapping reduction processes.

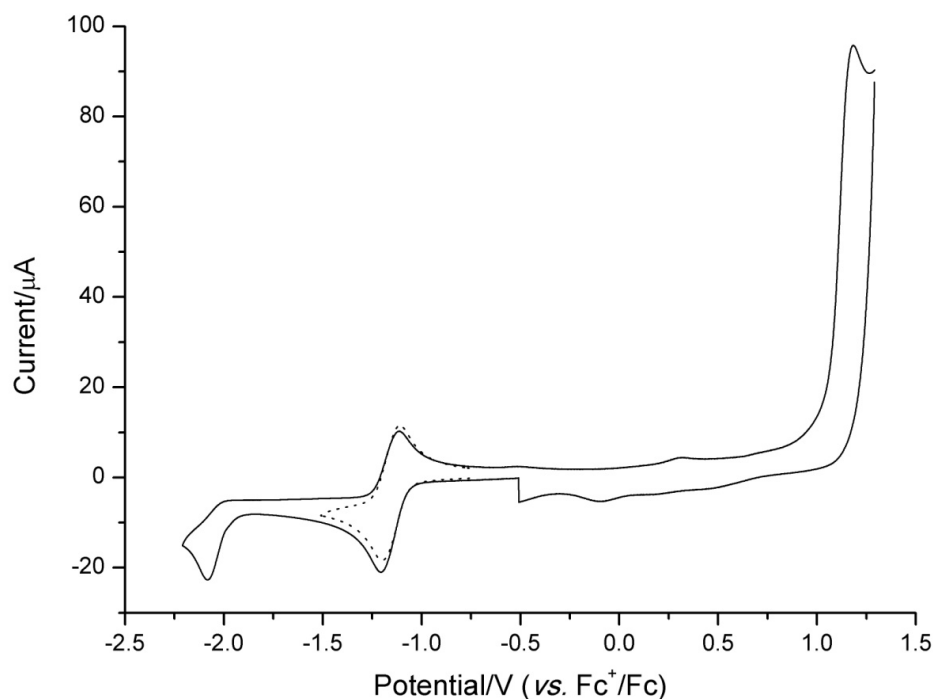


Figure S4. Cyclic voltammogram of **5** at RT in CH_2Cl_2 with $[\text{nBu}_4\text{N}][\text{BF}_4]$ (0.4 M) as supporting electrolyte ($E_{1/2} = -1.17$, vs. Fc^+/Fc).

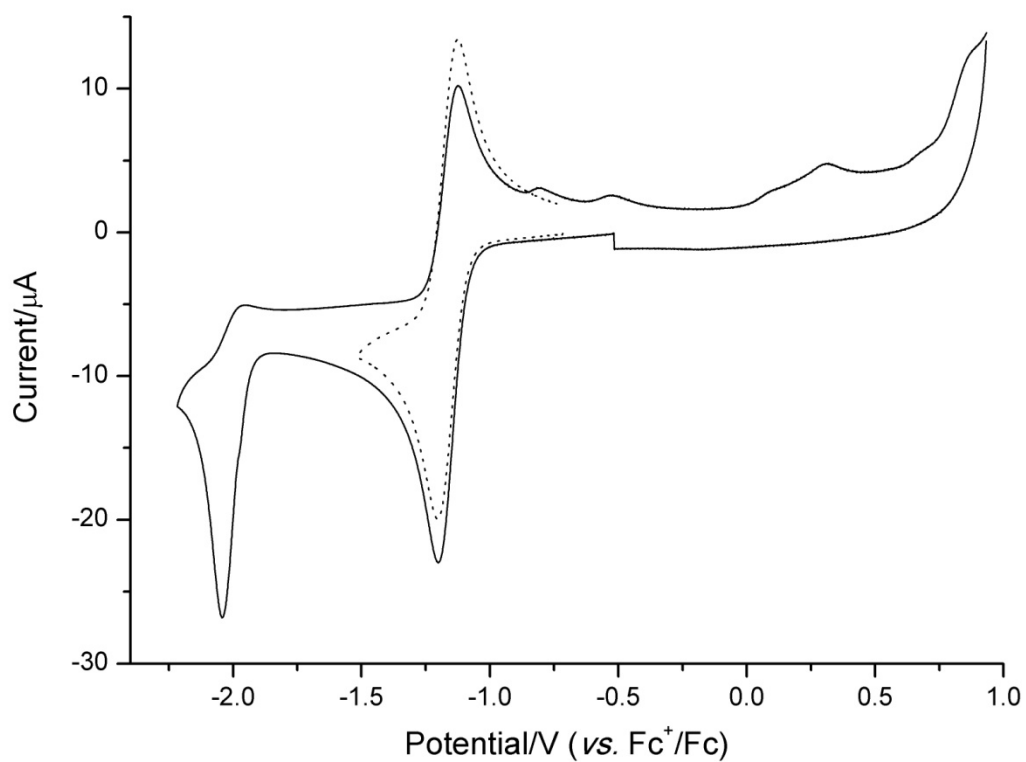


Figure S5. Cyclic voltammogram of **6** at RT in CH_2Cl_2 with $[\text{nBu}_4\text{N}][\text{BF}_4]$ (0.4 M) as supporting electrolyte ($E_{1/2} = -1.16$, vs. Fc^+/Fc).

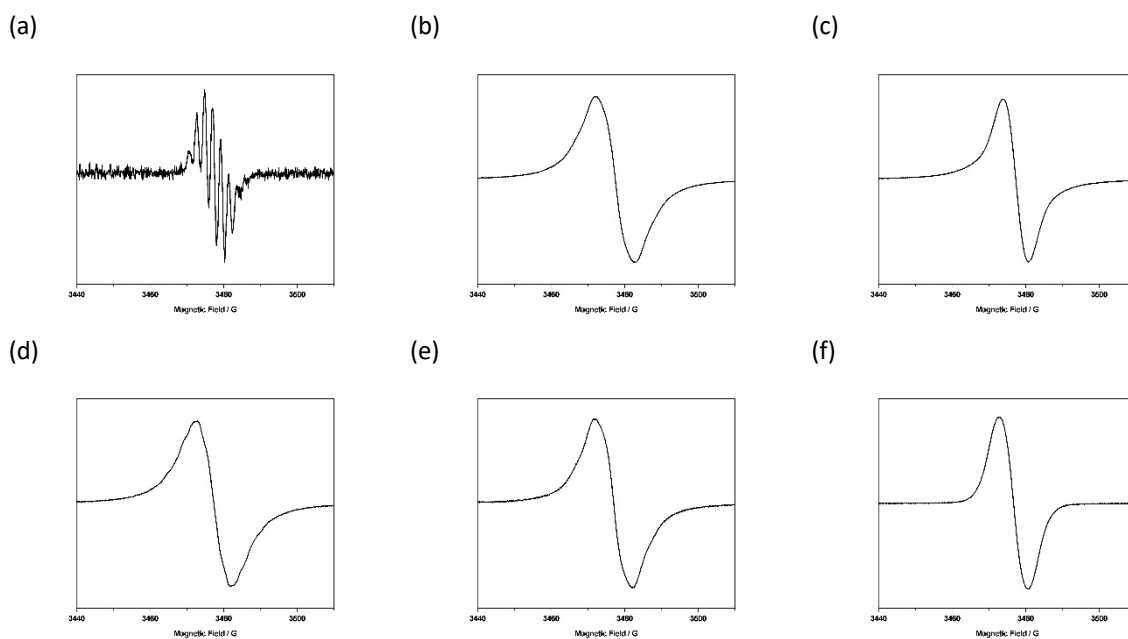


Figure S6. EPR spectra recorded at ambient temperature for solutions of a) residual spectrum formed on reduction of **1**, b) $[\mathbf{2}]^{2-}$; c) $[\mathbf{3}]^{3-}$; d) $[\mathbf{4}]^{2-}$; e) $[\mathbf{5}]^{2-}$; f) $[\mathbf{6}]^{2-}$ in CH_2Cl_2 with $[\text{nBu}_4\text{N}][\text{BF}_4]$ (0.4 M).

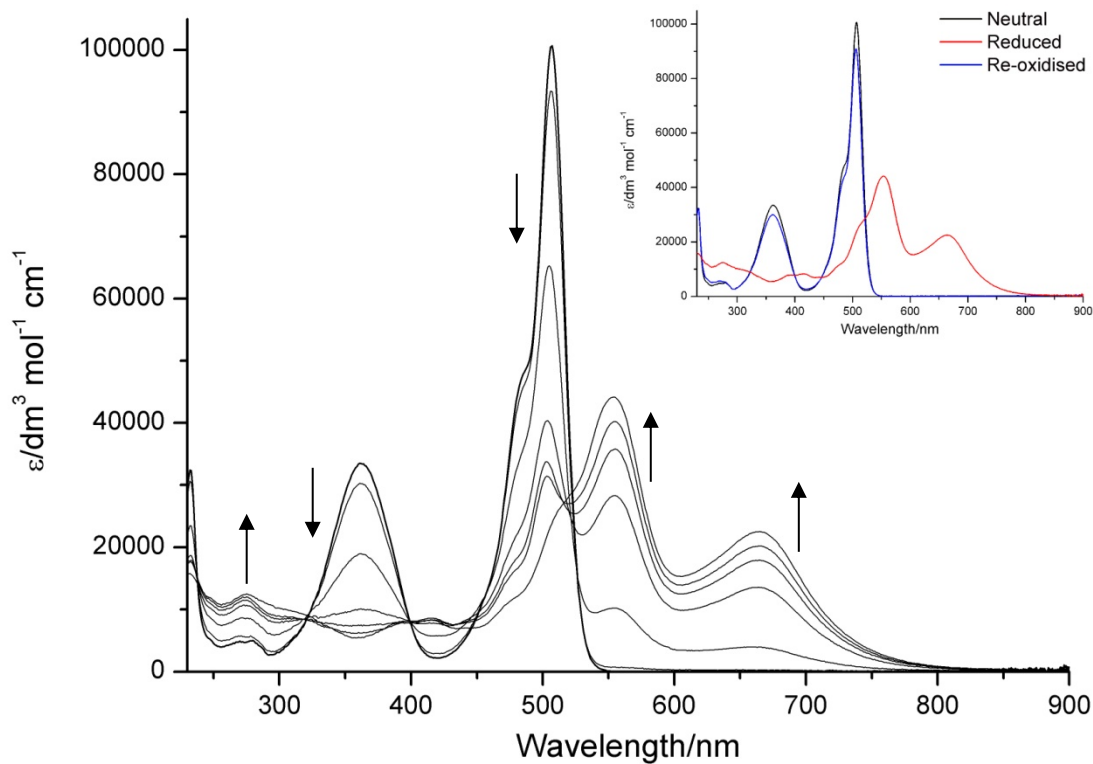


Figure S7. UV-vis spectroelectrochemistry of **1** in CH_2Cl_2 with $[\text{nBu}_4\text{N}][\text{BF}_4]$ as electrolyte at 243 K (applied potential from -0.10 V to -0.75 V).

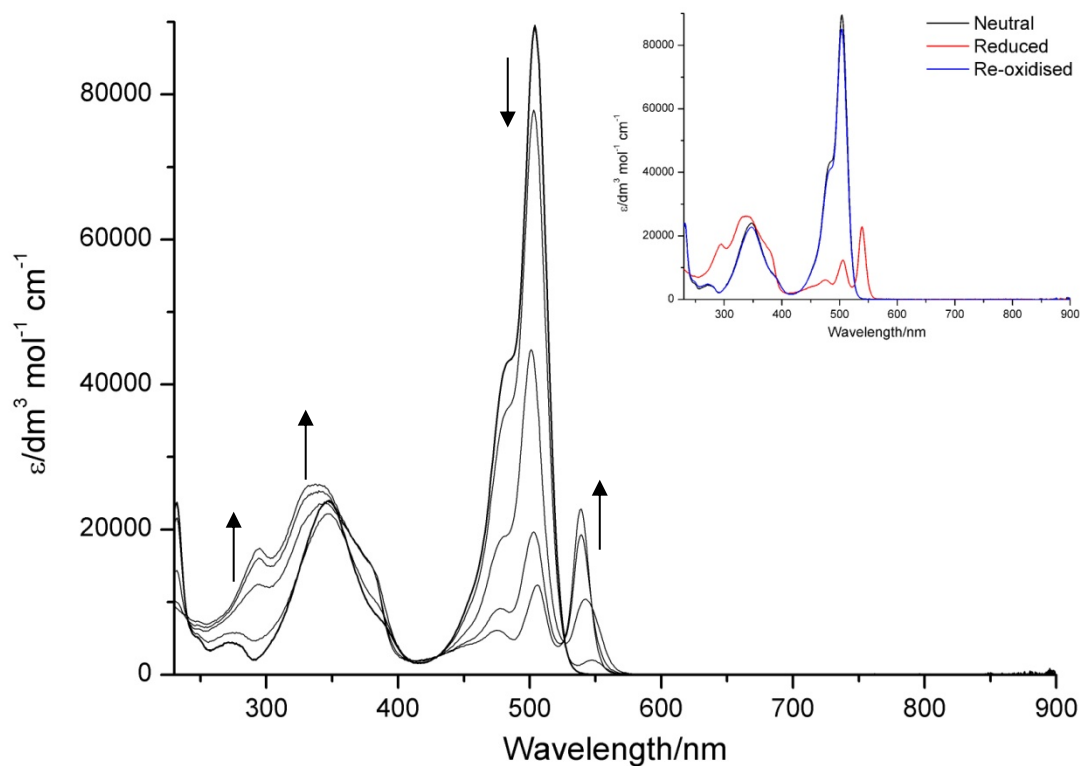


Figure S8. UV-vis spectroelectrochemistry of **2** in CH_2Cl_2 with $[\text{nBu}_4\text{N}][\text{BF}_4]$ as electrolyte at 243 K (applied potential from -0.10 V to -1.00 V).

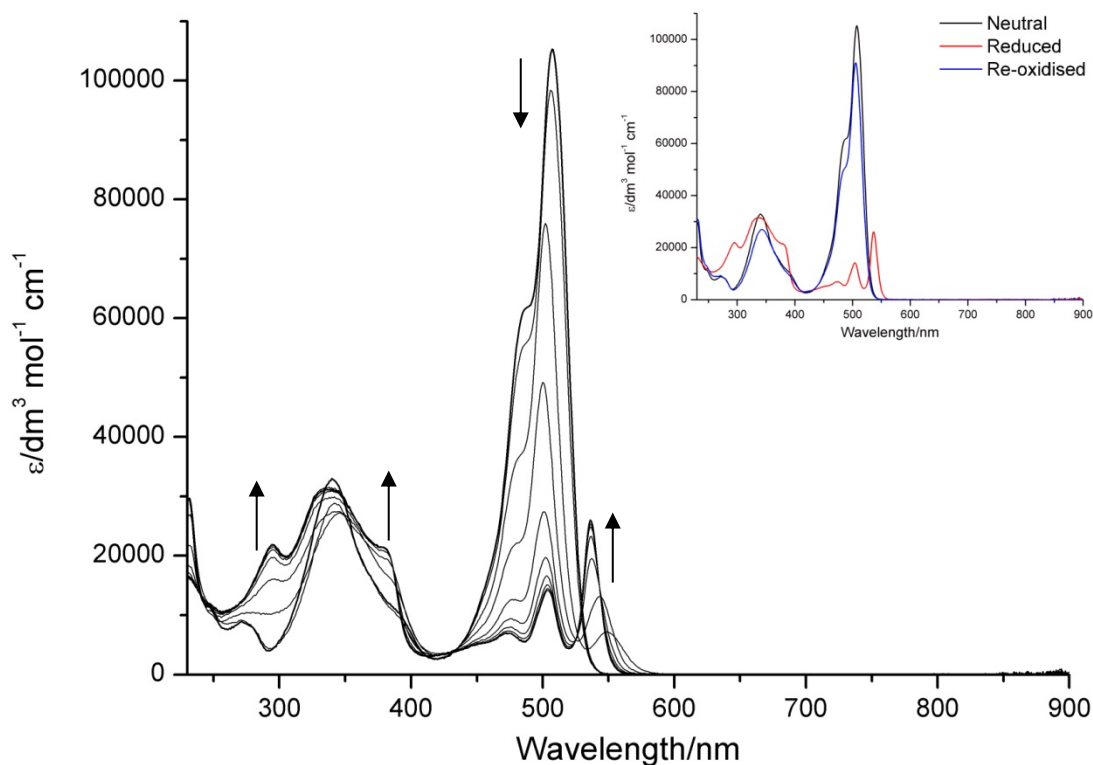


Figure S9. UV-vis spectroelectrochemistry of **3** in CH_2Cl_2 with $[\text{nBu}_4\text{N}][\text{BF}_4]$ as electrolyte at 243 K (applied potential from 0.00 V to -1.00 V).

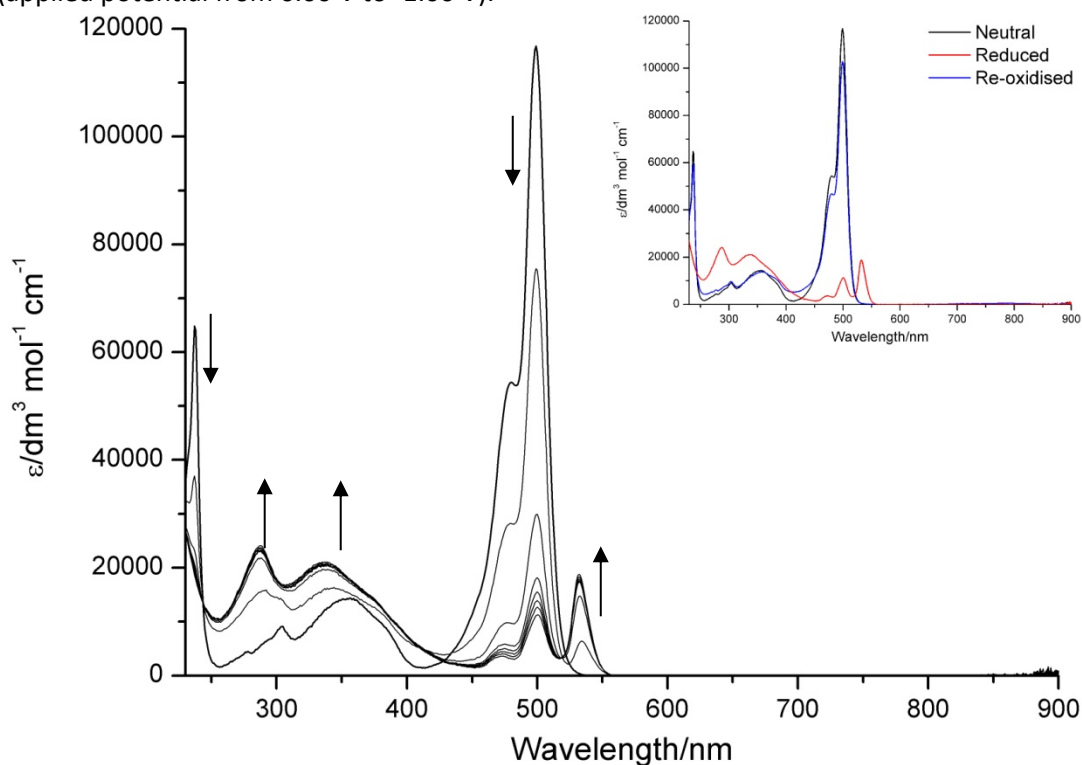


Figure S10. UV-Vis spectra of **4** in CH_2Cl_2 with $[\text{nBu}_4\text{N}][\text{BF}_4]$ as electrolyte at 243 K (applied potential from -0.5 V to -1.2 V). Arrows indicate change in spectra upon reduction of **[4]** to **[4]²⁻**.

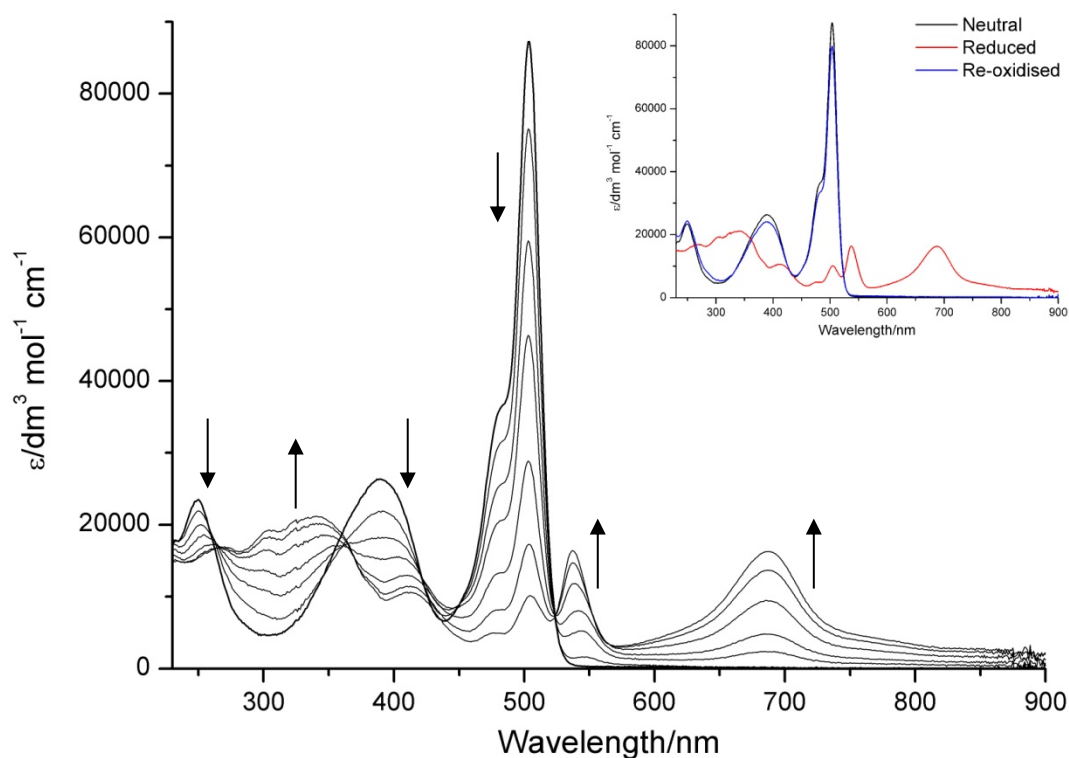


Figure S11. UV-Vis spectra of **5** in CH_2Cl_2 with $[\text{nBu}_4\text{N}][\text{BF}_4]$ as electrolyte at 243 K (applied potential from 0.0 V to -1.0 V). Arrows indicate change in spectra upon reduction of **[5]** to **[5]²⁻**.

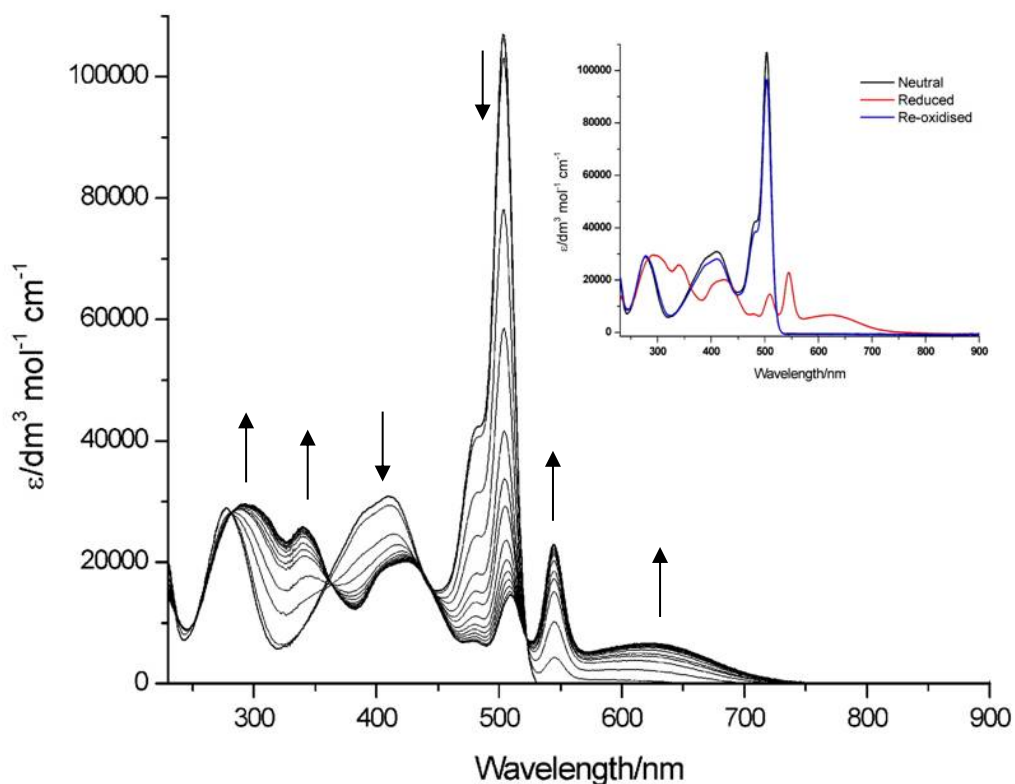


Figure S12. UV-Vis spectra of **6** in CH_2Cl_2 with $[\text{nBu}_4\text{N}][\text{BF}_4]$ as electrolyte at 243 K (applied potential from 0.0 V to -1.0 V). Arrows indicate change in spectra upon reduction of **[6]** to **[6]²⁻**.

Supplementary Figures for Fluorescence Spectroscopy

Compound	$\lambda_{\text{abs}}/\text{nm}$	$\lambda_{\text{em}}/\text{nm}$	$\Phi_{\text{F}}^{\ddagger}$	τ/ns
1	505	534	0.008	<2
2	503	525	0.027	<2
3	505	533	0.018	<2
4	498	516	0.87	9
5	498	523	0.011	<2
6	502	522	0.015	<2

Table S2. Summary of fluorescence data for **1-6**. Spectra recorded in CH_2Cl_2 at RT with excitation at 406 nm. ‡ Quantum yields were recorded using $[\text{Ru}(\text{bpy})_3]^{2+}$ (0.04 M in H_2O) as a standard.

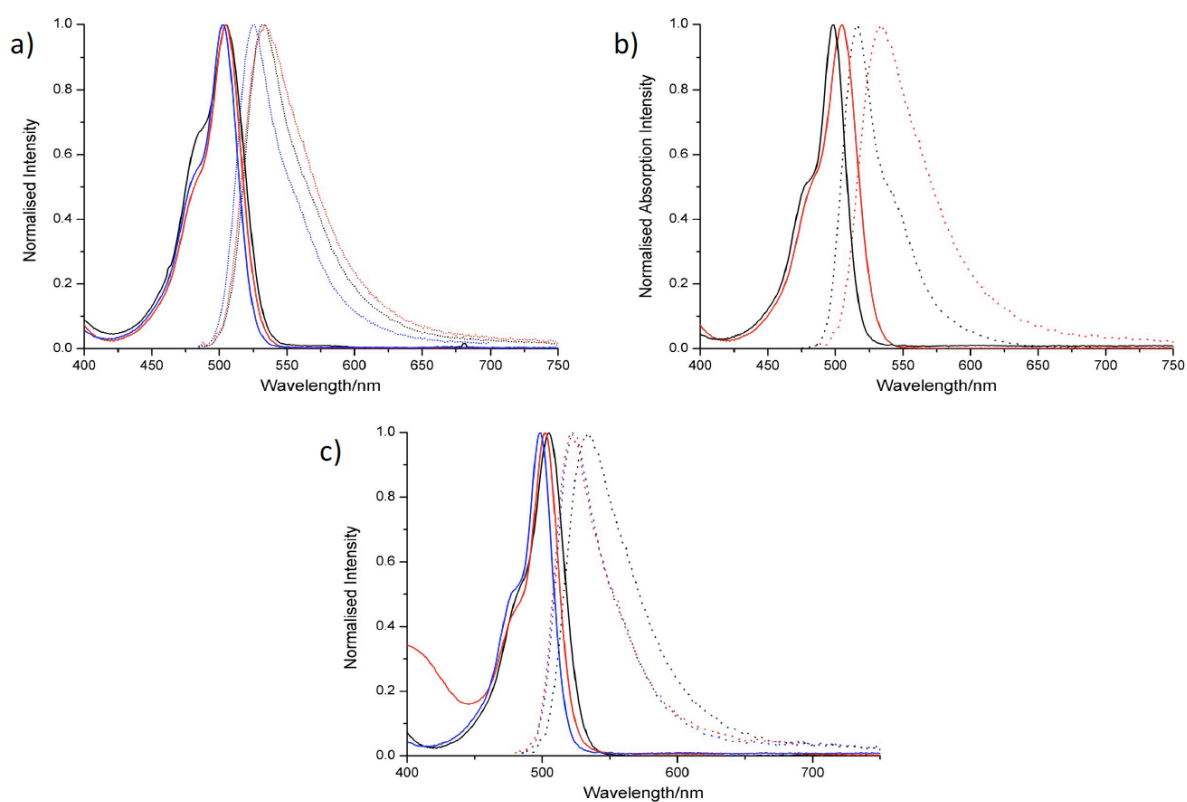


Figure S13. Normalised fluorescence data showing absorption (full lines) and emission (dotted lines) spectra for **1-6**. a) **1** - red; **2** - blue; **3** - black. b) **1** - red; **4** - black. c) **1** - black; **5** - blue; **6** - red.

DFT Geometry Optimized Structures and MO diagrams

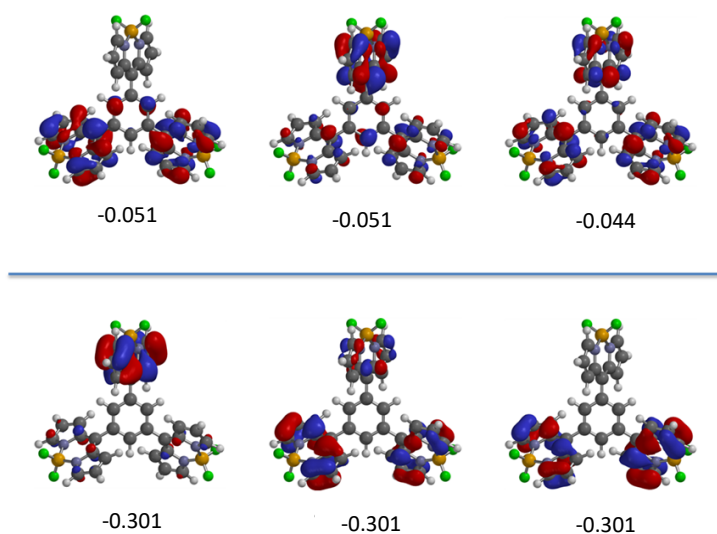


Figure S14. DFT calculated MO plots for **3** in the neutral ground state with the orbital energies in atomic units. The central line indicates the divide between the occupied and virtual MOs.

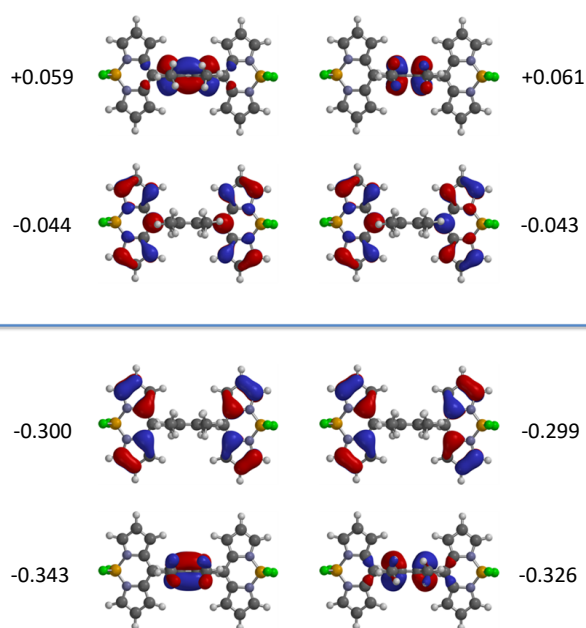


Figure S15. DFT calculated MO diagrams for **4** in the neutral ground state with the orbital energies in atomic units. The central line indicates the divide between the occupied and virtual molecular orbitals.

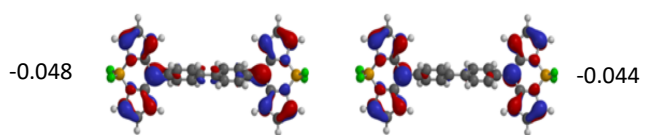


Figure S16. DFT calculated MO diagrams for **5** in the neutral ground state with the orbital energies in atomic units. Horizontal line indicates separation between occupied and unoccupied orbitals.

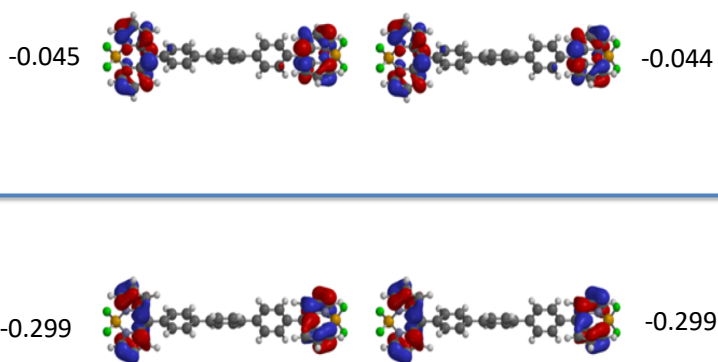


Figure S17. DFT Calculated MO diagrams for **6** in the neutral ground state with the orbital energies in atomic units. The horizontal line indicates the separation between occupied and unoccupied orbitals.

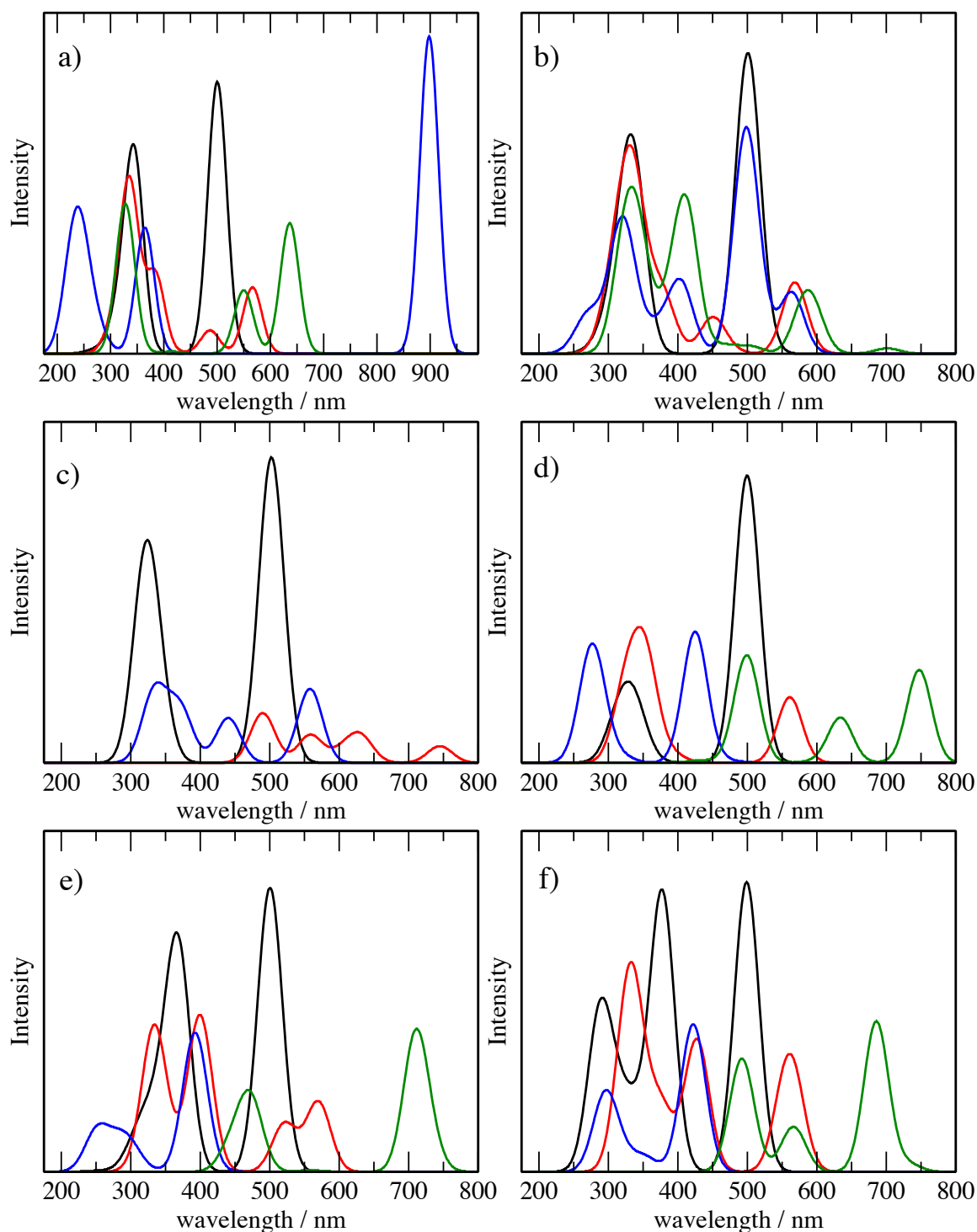


Figure S18. TDDFT electronic excitation spectra for a) **1**/[**1**]²⁻; b) **2**/[**2**]²⁻; c) **3**/[**3**]³⁻; d) **4**/[**4**]²⁻; e) **5**/[**5**]²⁻; f) **6**/[**6**]²⁻. Black: neutral, red: triplet, blue: closed shell singlet, green: open shell singlet. For **3**, black: neutral, red: doublet, blue: quartet. All calculations use continuum solvent model (dielectric constant=80).

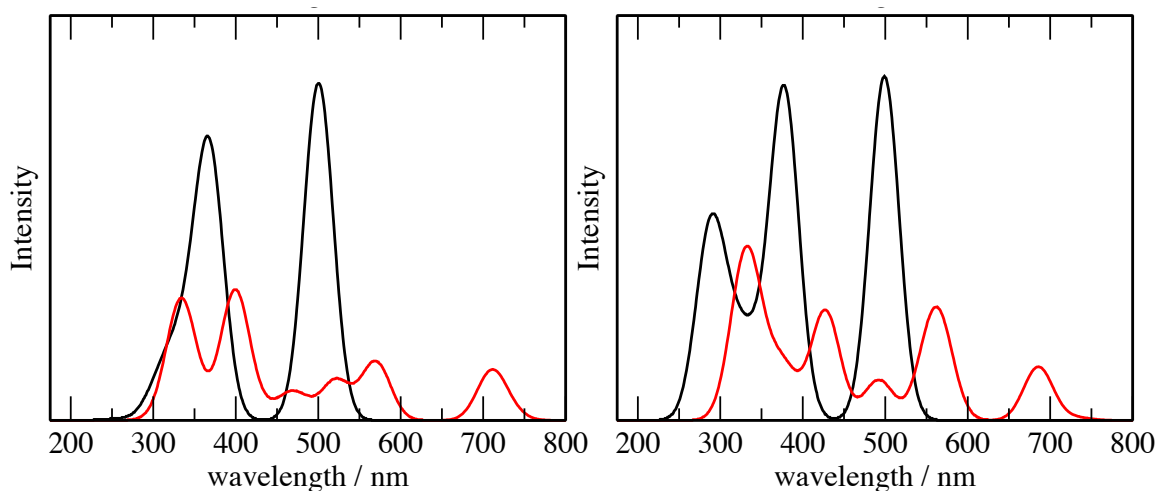


Figure S19. TDDFT electronic excitation spectra for left) $[5]^{2-}$ and right) $[6]^{2-}$. Each spectrum represents the profiles generated by hybrid spectra composing 2/3 triplet (black) and 1/3 open-shell singlet (red).

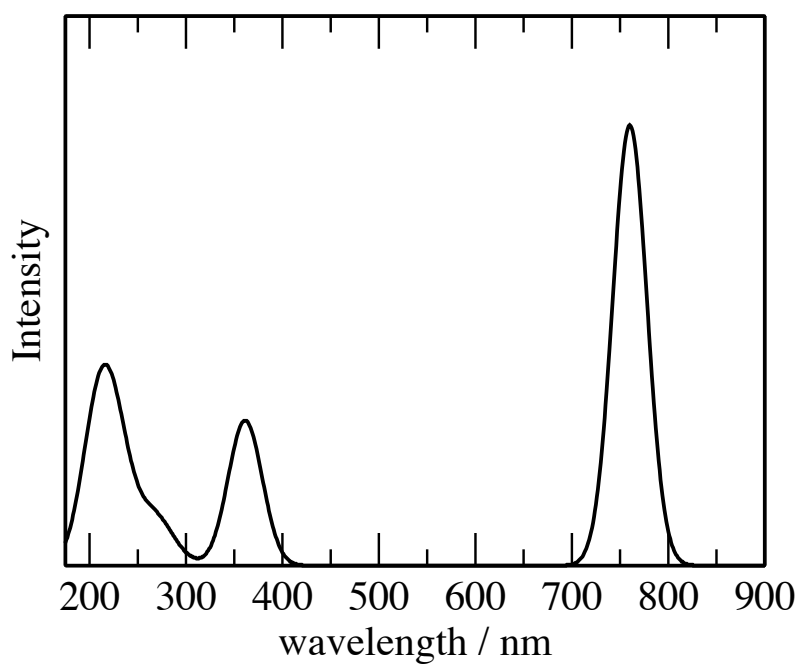
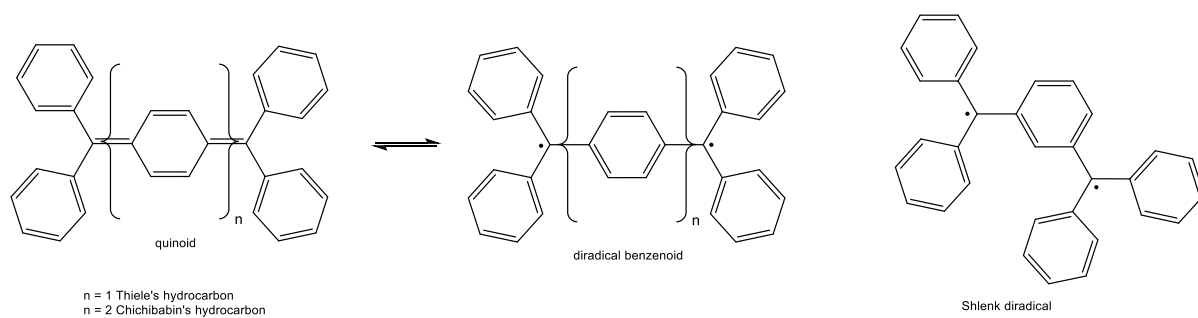
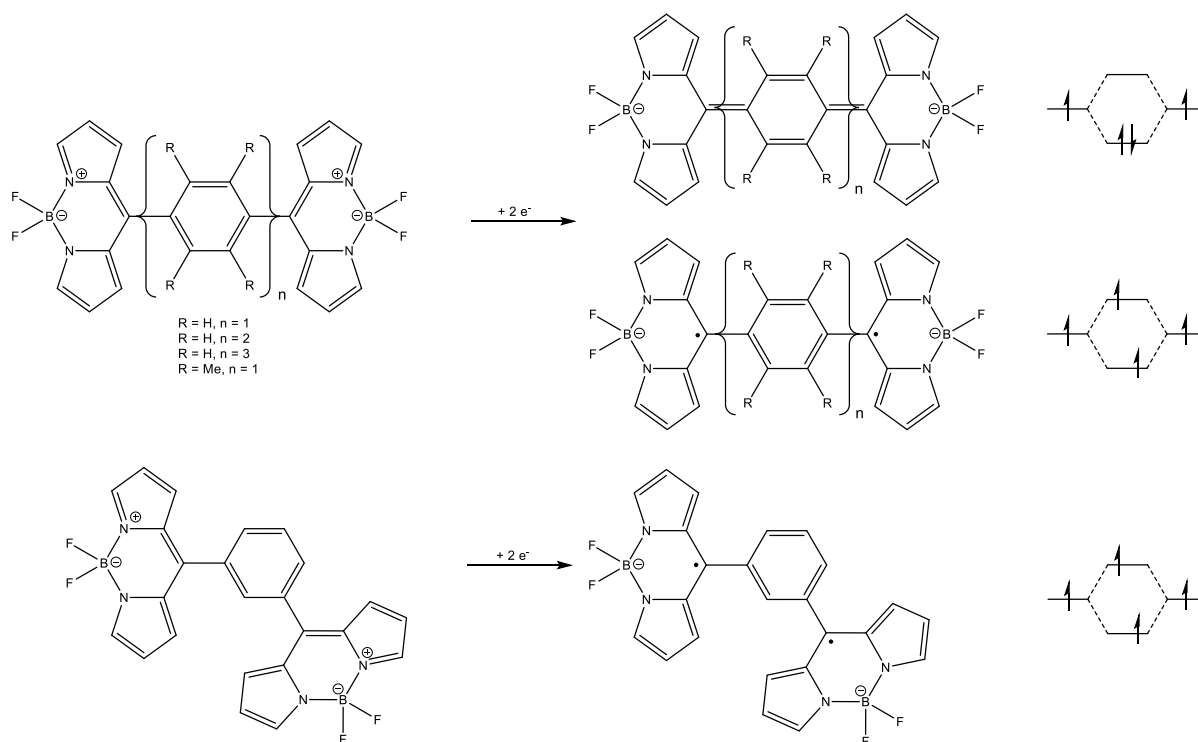


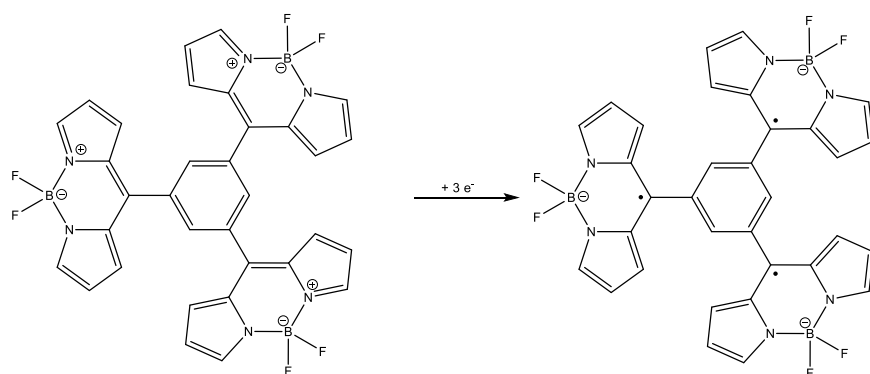
Figure S20. TDDFT electronic excitation spectra for the closed-shell singlet state of $[1]^{2-}$ using a flattened conformation. Calculations were performed on a molecule which was required to have a co-planar arrangement between the dipyrin and linking phenyl moieties.



Scheme S1. Representations of Thiele and Chichibabin quinoidal or a biradical benzenoidal forms and the Schlenk diradical.



Scheme S2. Representations of quinoidal or a biradical benzenoidal forms for $[1]^{2-}$ and illustration of how such resonance structures are not feasible for $[2]^{2-}$.



Scheme S3. Illustration of the potential arrangement of $[3]^{3-}$ and how quinoidal structures cannot be adopted.

References

- S1. M. Nichols, B. Fabre, G. Marchand, J. Simonet, *Eur. J. Org. Chem.*, **2000**, 9, 1703-1710.
- S2. M. P. Castaldi, S. E. Gibson, M. Rudd, A. J. P. White, *Chem. Eur. J.*, 2006, **12**, 138-148.
- S3. A. Belaissaoui, S. Shimada, A. Ohishi, N. Tamaoki, *Tetrahedron Lett.*, 2003, **44**, 2307-2310.
- S4. M. Fourmigue, I. Johannsen, K. Boubeker, C. Nelson, P. Batail, *J. Am. Chem. Soc.*, 1993, **115**, 3752-3759.
- S5. P. Gerstel, S. Klumpp, F. Hennrich, A. Poschlad, V. Meded, E. Blasco, W. Wenzel, M.M. Kappes, C. Barner-Kowollik, *ACS Macro Lett.*, 2014, **3**, 10-15.
- S6. A. W. van der Made, R. H. van der Made, *J. Org. Chem.*, 1993, **58**, 1262-1263.
- S7. Y.-T. Chan, X. Li, M. Soler, J.-L. Wang, C. Wesdemiotis, G. R. Newkome, *J. Am. Chem. Soc.*, 2009, **131**, 16395-16397.
- S8. O.V. Dolomanov, L.J. Bourhis, R.J. Gildea, J.A.K. Howard, H. Puschmann, *J. Appl. Cryst.* 2009, **42**, 339-341.
- S9. G.M. Sheldrick, *Acta Cryst.*, 2015, **A71**, 3-8.
- S10. G.M. Sheldrick, *Acta Cryst.*, 2015, **C71**, 3-8.
- S11. N. Mardirossian and M. Head-Gordon, *J. Chem. Phys.*, 2016, **144**, 214110.
- S12. A.T.B. Gilbert, N.A. Besley and P.M.W. Gill, *J. Phys. Chem. A*, 2008, **112**, 13164.
- S13. S. Hirata and M. Head-Gordon, *Chem. Phys. Lett.*, 1999, **314**, 291.
- S14. M. J. G. Peach , P. Benfield , T. Helgaker , and D. J. Tozer , *J. Chem. Phys.*, 2008, **128**, 044118
- S15. J. Tomasi, B. Mennucci and R. Cammi, *Chem. Rev.*, 2005, **105**, 2999.
- S16. Y. Shao et al, *Mol. Phys.*, 2015, **113**, 184.
- S17. K. Andersson, P.A. Malmqvist, B.O. Roos, A.S. Sadlej and K. Wolinski, *J. Phys. Chem.*, 1990, **94**, 5483.
- S18. H.-J. Werner, P.J. Knowles, G. Knizia, F.R. Manby and M. Schütz, *WIREs Comput. Mol. Sci.*, 2012, **2**, 242.